2018-01-15

Use of constrained focused waves to measure extreme loading of a taut moored floating wave energy converter

Hann, Martyn

10.1016/j.oceaneng.2017.10.024
Ocean Engineering
Elsevier

Ocean Engineering 148 (2018) 33–42

Contents lists available at ScienceDirect

Ocean Engineering

journal homepage: www.elsevier.com/locate/oceaneng

Use of constrained focused waves to measure extreme loading of a taut moored floating wave energy converter

Martyn Hann *, Deborah Greaves, Alison Raby, Ben Howey

School of Engineering, Plymouth University, UK

ARTICLE INFO

Keywords:
NewWave
Constrained NewWave
Wave impact
Survivability
Moorings
Floating bodies

ABSTRACT

This paper concerns experimental measurements of the interaction of a taut moored floating body, representing a point absorbing wave energy converter in survivability mode, with extreme waves. The extreme waves are modelled in four ways. NewWave theory is first used to generate focused wave groups of varying steepness. Steepness is shown to have negligible effect on peak mooring loads, but causes significant differences in the resulting motion. The NewWave group is then constrained into both regular and irregular background wave trains so that the floating body has a load history caused by previous waves when interacting with the focused wave group. It is shown that an independent focused wave group is insufficient to properly model the extreme response of the floating body. However differences between the target and measured constrained time series due to non-linear wave-wave interaction limited the potential benefits of this approach. Finally the results from these tests are compared with measurements taken using irregular waves without any deterministic focused wave groups present. This comparison found cases where the floats response was greater than during any of the constrained NewWave tests, indicating that the assumption made that NewWave will generate the largest response was incorrect in this case.

1. Introduction

Floating wave energy converters must be designed to withstand the largest waves experienced during storms of magnitude equal to their design condition. This forms part of a wave energy device's survivability criterion, part of the dual requirements of any marine energy device: the ability to extract energy in small to moderate seas, while surviving more extreme conditions (Barstow et al., 2008 p. 52). Achieving an understanding of the response to these extreme waves is important. Large degrees of uncertainty in the expected loads often lead to the use of conservative assumptions which can negatively influence the commercial viability of a device (O'Neill et al., 2006).

Most floating offshore wave energy converters are being designed to deploy in arrays. Spacing between individual devices within an array depends on many factors, including maximising power generation, provision of maintenance access and achieving an acceptable collision risk. For this last point it is important to be able to also predict the maximum expected displacement of devices during extreme events.

Both experimental and numerical techniques are used to model a device's response to extreme waves. In both cases a deterministic focused wave group based on NewWave theory is often used to generate a time series of an extreme wave. NewWave theory, as described by Tromans et al. (1991), models the statistically most probable surface elevation shape associated with the occurrence of an extreme wave crest with a specified exceedance probability (Pinna and Cassidy, 2004). NewWave theory has the advantage that it generates an extreme event within a relatively short time series when compared to relying on randomly occurring extreme events in an irregular time series of the sea state in question. The short time series means, in a correctly designed experiment, that all important wave-structure interactions occur before any significant influence from wave reflections from basin walls occur. The wave group generated by NewWave theory propagates into calm water. This and again the relatively short time series involved, means that NewWave focused wave groups are well-suited for proving validation data for computationally expensive computational fluid dynamic (CFD) models.

These advantages of using NewWave focused wave groups to measure extreme wave interactions have led to the approach being used in a wide number of applications. In the offshore environment extreme wave impacts on fixed cylinders relevant to a wide range of structures have been assessed both experimental and numerically using NewWave theory (Walker and Eatock Taylor, 2005; Ransley et al., 2013; Zang et al., 2010),

* Corresponding author.
E-mail address: martyn.hann@plymouth.ac.uk (M. Hann).

https://doi.org/10.1016/j.oceaneng.2017.10.024
Received 13 June 2017; Received in revised form 8 October 2017; Accepted 15 October 2017

while Stallard et al. (2009a) measured the forces on a vertical cylinder moving through a stationary fluid with a motion devised from NewWave theory. Rozario et al. (1993) successfully compared the loads predicted by NewWave on a North Sea oil platform with simulations of random seas. Westphalen et al. (2014) conducted Volume of Fluid and SPH CFD simulations of NewWave wave groups interacting with the Manchester Bobber wave energy device, comparing results to those from 70th scale experimental measurements (Stallard et al., 2009b; Weller et al., 2013). More recently NewWave theory has been used to investigate the impact of extreme waves in the coastal environment. Borthwick et al. (2006) measured wave kinematics of NewWaves impacting on a 1:20 beach plane, while Whittaker et al. (2017) measured wave runup of a plane beach.

Focused wave groups such as those generated by NewWave theory are used to represent the design load case for fixed structures (Stallard et al., 2009b). Their use as design cases for dynamic structures and devices is questionable however. When dynamic response to waves is expected, the response to a specific extreme wave will depend not only on the load induced by the wave, but the load history caused by the previous wave train (Pinna and Cassidy, 2004). This dependency is not investigated when testing with a single focused wave group. The device or structure in question has a stationary initial state and only interacts with the deterministic wave crests and troughs that made up the initial part of the focused wave group before interacting with the extreme central crest.

Constraining (or embedding) the NewWave within a random background sea state is an approach which allows the effect that a device or structures load history has on that device or structures response to a deterministic extreme event to be investigated. Introduced by Taylor et al. (1997), a Constrained NewWave (CNW) consists of a NewWave group which is constrained into an irregular background sea state with the same characteristic spectrum, such that the resulting time series is statistically indistinguishable from a randomly occurring wave train. The impact of the device's load history variation and the resulting distribution of the responses to the extreme wave can then be investigated by conducting multiple simulations or experiments with the focused wave group constrained into different random background time series.

Various numerical studies have concluded that using the CNW technique is a viable alternative to conducting simulations with random irregular wave time series. For example Cassidy (1999) and Cassidy et al. (2001) demonstrated the use of CNW to determine the short-term extreme response statistics of a Jack-up structure, using 5 NewWaves each constrained into 200 random backgrounds. Their results were found to be comparable to those found from 100 3 h simulations of random seas. Pinna and Cassidy (2004) conducted similar simulations on a fixed monopod platform using 100 CNW cases while Enderami et al. (2010) modelled the extreme response of a Jacket offshore platform using 200 CNW, both with ABAQUS. Both compared results with simulations of 3 h long irregular sea states and found that the maximum response were of a similar magnitude.

Bennett et al. (2012) report what they believed to be the first experimental use of CNW. They compared the use of an independent NewWave, CNW and an ‘optimised sea state’ to model the rigid body motions of a travelling ship in abnormal waves, where the optimised sea state requires an iterative adjustment of the phases in a random sea state so that a target extreme wave occurs. The three different approaches to generating ‘abnormal’ sea conditions were tested for three JONSWAP sea states with increasing significant wave height. Discrepancies between the target and generated wave were reported for the CNW, which was considered to be potentially due to the combination of two wave spectra. Göteman et al. (2015) constrained NewWave into regular waves when measuring the wave load on a point-absorbing wave energy device. The focused wave was constrained into different phase locations within regular waves with four different periods, resulting in 32 cases in total. A correlation between wave height and measured mooring force is reported.

This paper presents a systematic study into the experimental use of independent NewWave and CNW in the investigation of a moored floating body's response to an extreme wave. Results from four sets of experiments are reported and compared. In the first series the interaction of the moored floating body with an independent NewWave focused wave group was measured, along with the interaction with three other focused groups of increasing steepness. In the second series 24 constrained NewWave cases were tested within two regular background waves. In the third series the NewWave was constrained into 180 unique irregular wave backgrounds. The final experimental series consisted of two 3 h long irregular wave time series, without any NewWave group present. A single sea state, representing a 100 year return period at Wave Hub, a wave energy test site of the North Cornwall Coast (UK) was used throughout. The differences between the maximum mooring loads and surge measured during the four set of experiments are specific to the float geometry, mooring arrangement and wave conditions tested here. However by comparing the results from the four different sets of experiments conclusions are drawn and recommendations made about the application of independent and constrained NewWave to the experimental determination of the extreme response of a moored floating body.

2. Experimental methodology

The floating body tested was the same as used in Hann et al. (2015), but with an altered mooring arrangement (Fig. 1). It is a 0.5 m diameter floating body, consisting of a hemisphere and 0.25 m high cylinder, with a dry mass of 43.2 kg and made from steel with a concrete ballast. The floats centre of mass was about the central axis of the float, 0.319 m from the top of the cylinder. Moments of inertia were $I_{xx} = I_{yy} = 1.61$ kg m^2 and $I_{zz} = 1.25$ kg m^2. A single taut mooring was used consisting of 1.38 m of 3 mm diameter Dyneema® rope (spring constant, $k \approx 35$ N/mm) in series with a 12.5 mm diameter linear spring ($k = 0.066$ N/mm), which provided the mooring's extension. The initial and maximum rated length of the spring was 0.63 m and 1.145 m respectively. In still water the spring was extended by 0.31 m. End stops, consisting of 4 Dyneema®

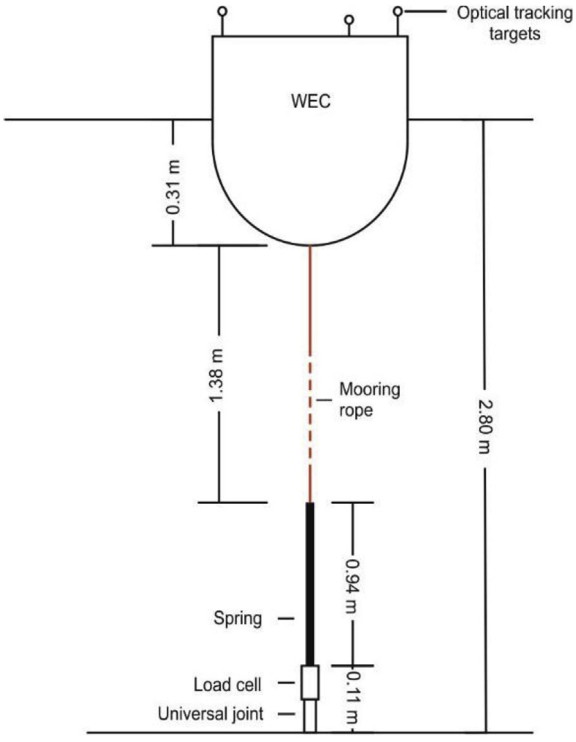

Fig. 1. Model set-up and instrumentation. The discrepancy of 0.06 m between 2.8 m water depth and the total length of the individual mooring components shown and submerged float is due to 3 × 0.02 m long shackles, located between the spring and load cell, the spring and mooring rope and the mooring rope and float.

ropes around the spring, were installed to prevent the spring from being overextended. Throughout these experiments the spring was never extended to its maximum length, and as such these end stops were never reached.

Mooring loads were measured using a 500N load cell (40 mm high, 44 mm diameter) attached in line with the mooring to the tank floor via a 74 mm long, 22 mm diameter universal joint (Fig. 1). Three 0.02 m shackles connected the spring to the load cell, the spring to the mooring line and the mooring line to the float. Mooring loads are reported as the difference between the dynamic mooring load and the moorings static, equilibrium load (i.e. the additional load). An optical tracking system was used to record the motion of the model in 6 degrees of freedom about a global coordinate system. The reported motions are of the centre of mass of the model. The averaged measured residual in the optical tracking system was ±1.15 mm. Decay tests conducted on the moored float identified the system to have resonance frequencies of 0.93 Hz in heave, 0.75 Hz in pitch and 0.07 Hz in surge. Although the floating body and mooring are not representative of a specific full scale wave energy device, the experiments are considered to be conducted at 50th scale based on the scaling of the wave conditions (section 3.1).

Measurements were conducted in a 35 m × 15.5 m ocean basin at Plymouth University's COAST laboratory. The variable floor depth was set at 2.8 m. The facility has 24 2.0 m deep hinged wave paddles across one side of the tank. Wave reflections are reduced using a parabolic beach and the wave paddle's active absorption.

The model was moored, in its resting position, along the centre line of the basin, 18.8 m from the front of the wave paddles. A series of 9 resistance type wave gauges were positioned along a line 1.46 m away from the tanks centre line. The location of these gauges relative to wave paddles and the model are given in Table 1.

Wave gauge 6 was positioned so that it was approximately aligned with the front face of the model. All waves generated in this sequence of measurements were long crested and normally-incident. It is assumed that the waves impacting the model are identical to those recorded 1.46 m to the side of the model. Two further wave gauges were positioned on the tank's centre line in line with wave gauge 2 and 3 to confirm this assumption.

3. NewWave generation

3.1. Independent NewWave

The first series of tests measured the response of the floating body to four independent focused wave groups. The first was a NewWave group generated using a Pierson-Moskowitz (PM) spectrum with a peak period and wave height based on 50th scale hindcast data (Halcrow, 2006 p. 19) for a 100-year return period storm at Wave Hub, a wave energy test facility off the north Cornwall coast in the south west of the UK ($T_z = 1.99$ s, $H_s = 0.288$ m).

The theoretical amplitude of the central crest of the NewWave, *A,* was set to be the largest expected amplitude in *N* waves, as given by:

$$A = \sqrt{2m_o \ln(N)}, \quad (1)$$

where m_o is the zeroth moment of the spectrum (Hunt-Raby et al., 2011). Based on Hunt-Raby et al. (2011), *N* was set to 1000, representing the approximate number of waves expected in a 3 h sea state, resulting in a target crest amplitude of 0.267 m. For the second, third and fourth focused wave groups this target crest amplitude was maintained, while the peak period of the spectrum used to generate the NewWave was progressively increased to increase the crest steepness (*kA*). The peak frequency multiplication factor of each of the wave groups tested are given in Table 2.

The theoretical focus location of each wave group is wave gauge 6, the approximate location of the front of the model when stationary. Fernández et al. (2014) discuss various reasons why focused waves do not generally come to focus at the theoretical focus location and time, as defined by linear theory. This includes non-linear wave-wave interactions within the wave packet (as investigated by Baldock et al. (1996)) creating components that do not satisfy the linear dispersion relation. As used by Baldock et al. (1996) and Ning et al. (2009), a trial and error process was used to adjust the theoretical focus location of the wave group to achieve focus at the required location (±0.05 m). The wave group was judged to be in focus when the surface elevation time history was symmetrical i.e. the troughs on either side of the main crest had the same magnitude. Fig. 2 plots the difference between the adjusted theoretical focus location and the target/actual focus location against the theoretical crest steepness. An approximate linear relationship can be observed, indicating the increasing influence of non-linear effects as wave steepness increases.

3.2. Constrained NewWave

The CNW approach potentially provides a means to investigate the effect that a device's load history, as generated by previous waves, has on the response of the float to a specific extreme wave. The NewWave previously tested as an individual focused wave (S1) was constrained into 24 regular wave and 180 irregular wave time series. The methodology used to generate the CNW time sequence was based on that used by Cassidy (1999) and Bennett et al. (2012). Fig. 3 presents an example of this embedding procedure for one of the irregular cases, showing the initial random wave sequence, the initial independent NewWave and the resulting CNW.

The 24 regular CNW cases were generated by constraining the NewWave into 12 different phase locations within the time histories of two regular waves with frequencies of $f_1 = 0.38$ Hz and $f_2 = 0.53$ Hz. Both had a wave height of 0.204 m. This wave height is equal to $H_s/\sqrt{2}$, where H_s is the significant wave of the 1:100 year wave from which the NewWave was generated (McCabe and Aggidis, 2009; Blanco et al., 2015).

Varying the phase location at which the NewWave was constrained into the 2 regular waves systematically alters the floating body's motion at the point the focused wave interacts with the model. The phase location was varied from −150° to 180° in 30° intervals. Fig. 4 shows the NewWave constrained so the central crest occurs at a phase of 0°, 90° and 180° within the regular wave.

Each of the 180 different irregular background sea states into which the NewWave was constrained were 120 s long. The NewWave's were

Table 2
Measured properties of focused wave groups.

Case	Peak frequency multiplication factor	*A* (measured) (m)	Δ*t* (sec)	*kA*
S1	1.00	0.273	1.11	0.227
S2	1.09	0.280	1.05	0.260
S3	1.18	0.286	1.00	0.289
S4	1.26	0.318	0.90	0.397

Table 1
Location of wave gauges (WG) relative to wave paddles ($x_{paddles}$) and the centre of the model's resting position (x_{model}).

WG #	1	2	3	4	5	6	7	8	9
$x_{paddles}$ (m)	13.27	15.24	17.52	17.85	18.19	18.56	18.90	19.25	19.61
x_{model} (m)	−5.53	−3.56	−1.28	−0.95	−0.61	−0.24	0.10	0.45	0.81

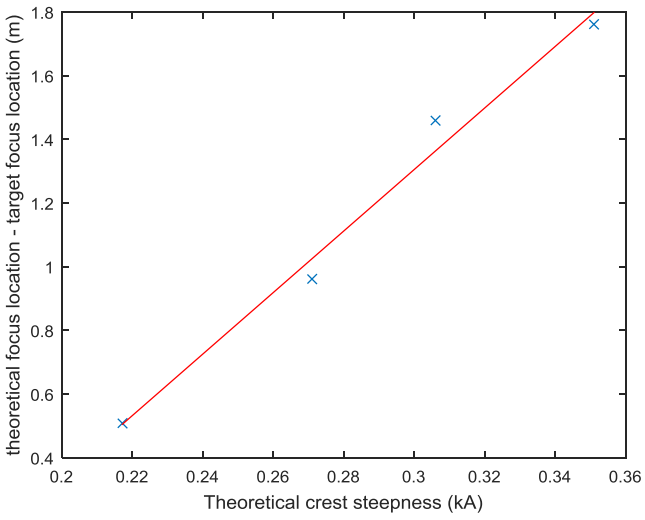

Fig. 2. Difference between theoretical focus location and target focus location.

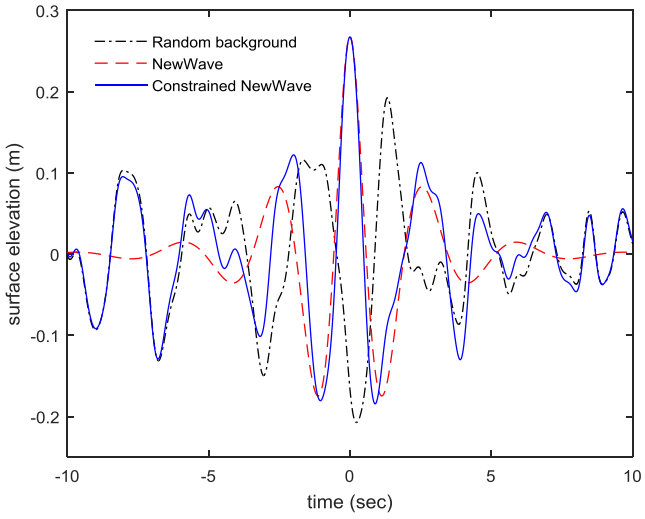

Fig. 3. Example of constrained NewWave.

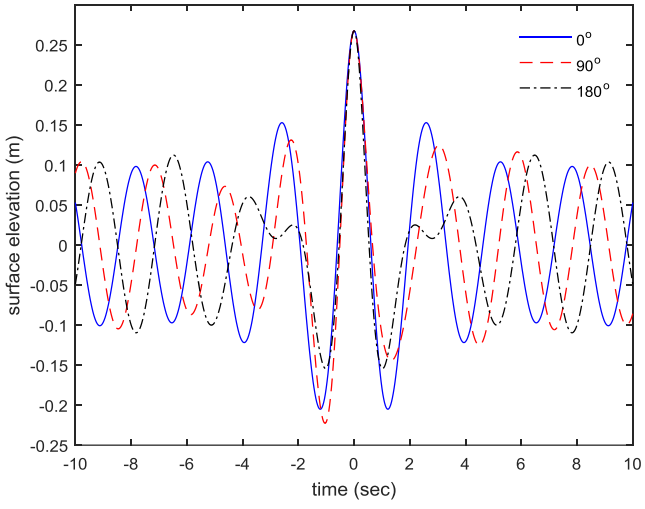

Fig. 4. Focused wave embedded into regular wave f_1 at a phase of 0°, 90° and 180°.

constrained such that the main crest occurred at 60 s. The background sea states were formed by generating two 3 h long irregular wave time series and splitting each of these into 90, 120 s sections. The two 3 h long time series were generated using a Pierson-Moskowitz spectrum and the same T_z and H_s values as used to generate the NewWave. Each of the 180 constrained NewWave time series were used as an input into the basin's wave generation software, with the theoretical focus location set to be the location of the front face of the model in its static location. Unlike with the four individual focused wave groups, it was not practical to use a trial and error approach to adjust the theoretical focus location of the 24 regular and 180 irregular constrained cases to achieve an improved focus.

4. Error assessment

4.1. Repeatability

The repeatability of the wave generation was assessed by repeating 1 of the 180 irregular constrained cases six times. Fig. 5 shows the measured wave at WG6 of these 6 repeats around the CNW. The average RMSE between the 1st wave and the following 5 repeats wave, excluding the first 20 s of the time series, was 0.012 m, indicating a good level of repeatability in wave generation.

A similar level of repeatability was observed in the mooring loads, with an average RMSE value between the first measurement and the following 5 repeats of 0.79 N, compare to an average peak load of 18.42 N.

4.2. Mooring extension and load comparison

The extension of the mooring has been calculated by translating the optical tracking system measurements to the model's mooring attachment point. Plots of this measured mooring extension against the measured mooring load for all 180 irregular CNW cases generated an average gradient of the line of best fit of 0.065 N/mm. This was consistent with the measured spring constant of the mooring spring. The average coefficient of determination (R^2) for these lines of best fit was 0.981.

The same measurements are presented in Fig. 6 for the peak loads and mooring extensions generated by the embedded wave in the 180 irregular CNW experiments. The line of best fit's gradient is also 0.065 N/mm with a coefficient of determination (R^2) of 0.966. Although this fit is less good, it still suggests that the spring remained linear and within its elastic regime during when the model was hit by the CNW.

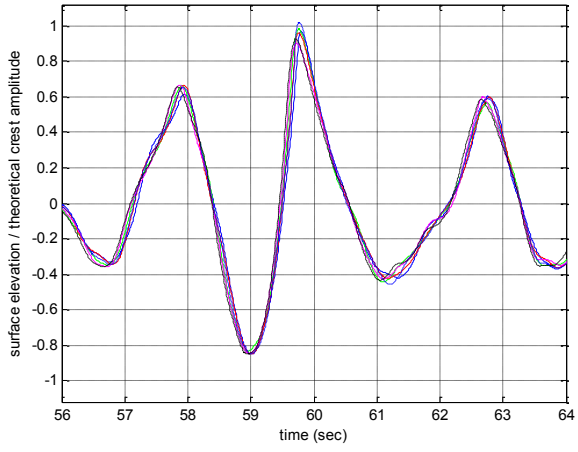

Fig. 5. Results of six repeat wave measurements, of a single irregular wave CNW case.

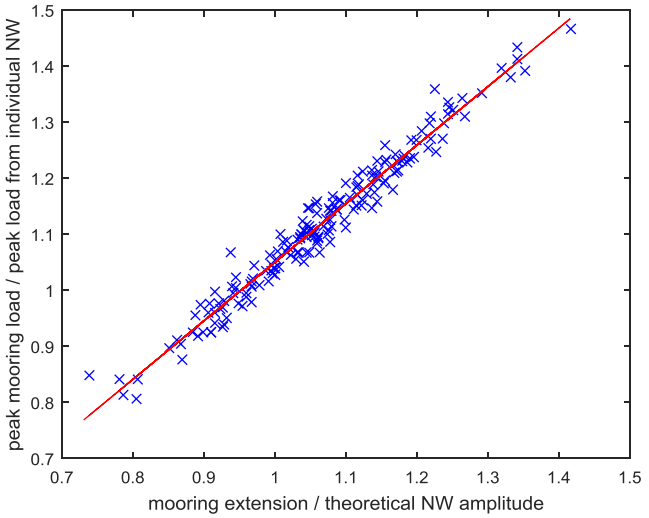

Fig. 6. Normalised peak mooring load plotted against the corresponding mooring extension.

5. Independent focused wave results

Fig. 7 shows the measured time history of the 4 independent focused wave groups. The measured main crest amplitude is presented in Table 2. The crest amplitude progressively increases as steepness increases, with the percentage difference between measured and target amplitude increasing from 2.2% to 19.1%. The wave troughs immediately preceding and following the main crest are, assuming linear wave theory, also expected to have the same elevation across the four wave groups. Fig. 7 shows that as wave steepness increased the measured group troughs were actually progressively less deep than the target waves. This observed behaviour of the main crest and troughs is in agreement with that investigated by Ning et al. (2009), who concluded that this is due to non-linear wave-wave interactions (particularly 3rd order).

Table 2 also presented the measured wave steepness. The same 4 wave groups were tested in Hann et al. (2015), where wave number k was calculated from the peak frequency of the measured wave group, assuming linear wave theory. Here wave number (k) is calculated based again on the assumption of linear wave theory but with a wave period taken to be twice the difference between the central wave crest and the preceding wave trough ($2\Delta t$). This was done to allow direct comparison with the steepness of constrained NewWaves measured in later test series.

Fig. 8 presents the mooring loads measured during the individual

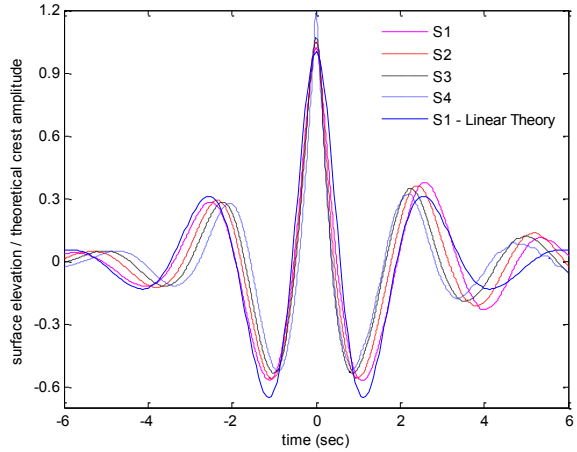

Fig. 7. Measured focused wave groups at focus location (WG6).

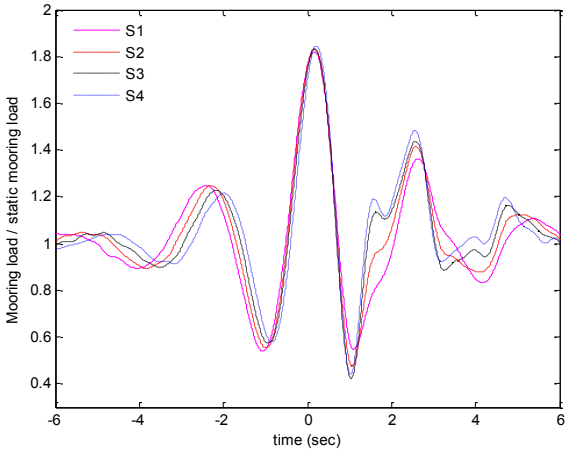

Fig. 8. Mooring loads resulting from focused wave groups of increasing steepness.

focused wave tests. Mooring load has been normalised with respect to the static mooring load. Overall peak load increased with wave steepness. However this load increase was only 1.3% between S1 and S4, compared to a 16.5% increase in crest elevation and a 74.9% increase in wave steepness. There was also no appreciable difference in the peak load generated by S2 and S3, with the generated loads lying between that generated by S1 and S4. This trend matches that observed in Hann et al. (2015) where snatch loading, generated when a taut mooring with reduced capacity compared to the one used in these tests reached its end stop, was only observed to increase by 4.7% as steepness increased between the same four wave groups. The difference in the mooring load peak subsequent to the largest peak, at around 2.6 s, increases to 8.8% between S1 and S4. This increase was monotonic in nature, with the load progressively increasing with wave steepness.

The corresponding motions of the float are presented in Fig. 9. No relationship was observed between focused wave group steepness and the peak in heave generated by the central wave crest, with the largest peak generated by S2 and the smallest by S4. However larger differences and monotonic increases with respect to wave group steepness are observed in surge and pitch. A 10.4% increase between S1 and S4 is

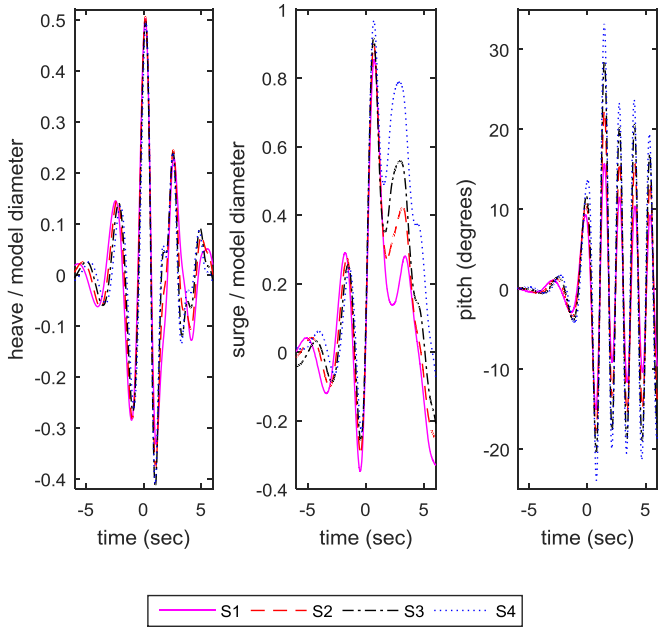

Fig. 9. Heave, surge and pitch response of taut moored floating body resulting from focused wave groups of increasing steepness.

observed in the peak in surge directly caused by the central wave crest of the focused wave, increasing to a 172% difference in the following peak. The magnitude of pitch for the first peak that followed interaction with the central wave crest demonstrated a 111% increase between S1 and S4.

These results indicate that the steepness of the focused wave crest does not significantly affect the mooring load directly generated by this crest. However the deviation in the float's surge and pitch response with changing wave steepness would result in an increased deviation in the mooring load measured between the 4 cases if there was to be an identical second wave later in the time series. This indicates the need to consider the effect of previous waves when modelling the effect of an extreme wave as even small changes in the previous wave history could result in the float being in a significantly different location and motion state when the extreme wave arrives.

6. Regular constrained NewWave results

Theoretically the CNW should have the same crest amplitude regardless of the background sea state it is embedded into (Fig. 4). However this approach is based on linear theory and does not take into account higher order wave-wave interactions that occur as waves propagate from the paddles to the focus location. Fig. 10 shows how the measured central crest amplitude changes relative to the phase location in the regular wave at which it is constrained. A clear relationship between the phase position and the generated crest amplitude can be observed.

As can be observed in Fig. 4, the trough preceding the central crest of the CNW changes slightly in both magnitude and time depending on the phase position in the regular wave into which it is constrained. This affects the steepness of the CNW. Fig. 11 shows how both the target and measured central crest steepness changes with phase position. The difference between the target and measured steepness changes with both the embedded phase position and the frequency of the background regular wave.

Tests were conducted with regular CNW as a means to systematically alter the position and motion of the model at the time where it interacted with the NewWave group. However the observed differences between the target and measured central crest amplitude and steepness make it difficult to separate these effects from those of changing the models position and motion on its response to the NewWave group. Fig. 12 presents how the peak mooring load generated by the regular CNW changes with the phase location.

In Fig. 13 the same load is compared to the measured amplitude of the central crest of the CNW. A strong correlation can be observed between

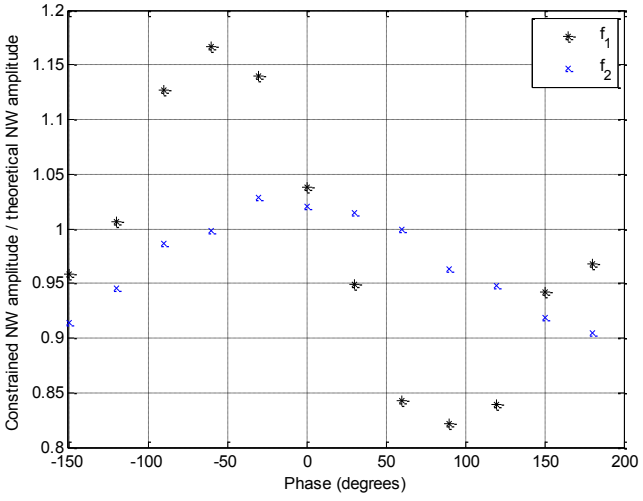

Fig. 10. Measured amplitude of the CNW central crest.

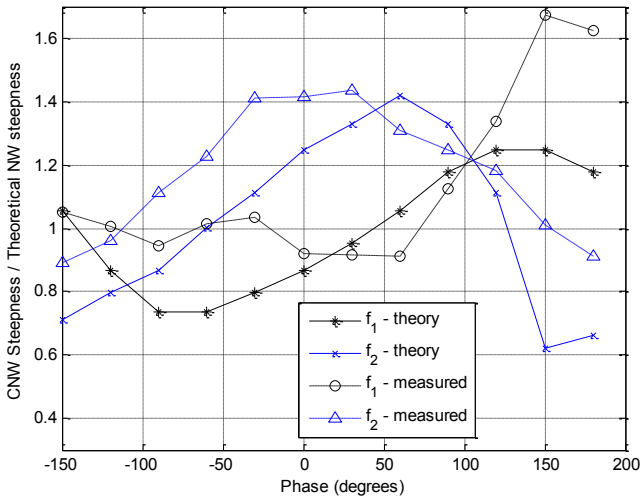

Fig. 11. Target and measured CNW crest steepness.

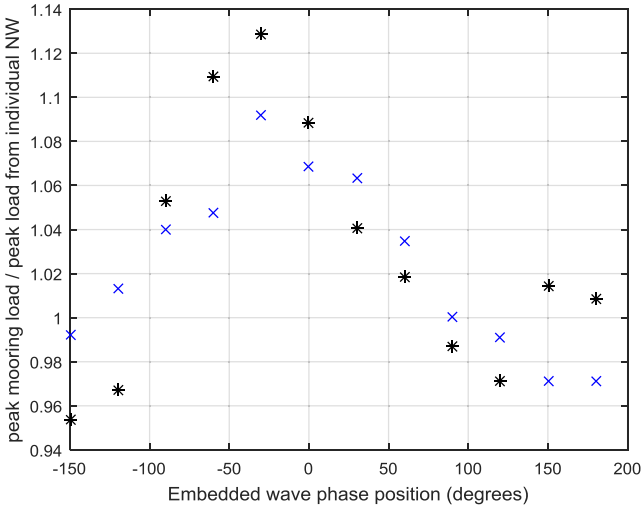

Fig. 12. Variation of peak mooring generated by the CNW with phase position.

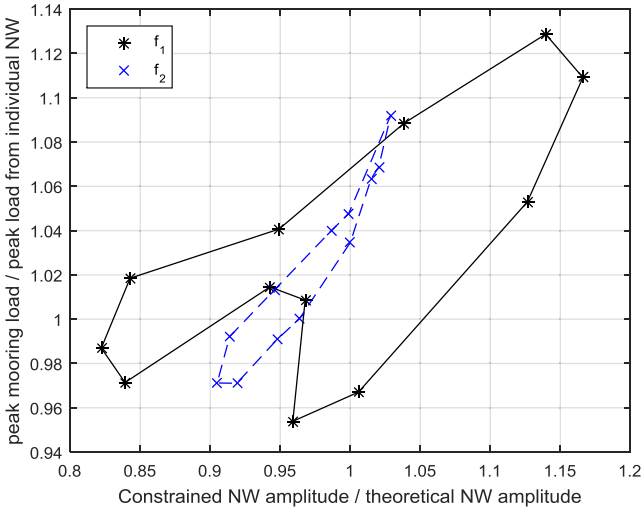

Fig. 13. Variation of peak mooring load generated by CNW with measured NewWave crest amplitude. Plotted lines link neighbouring phase locations.

amplitude and load for f_2, however a much weaker correlation is observed for f_1 (the R^2 value of a line of best fit is 0.54 for f_1 as compared to 0.87 for f_2). This suggests that either the previous motions generated by regular wave f_1 have a greater influence than for f_2 on the load generated by the CNW, or that the larger range over which the CNW amplitude varies in f_1 has resulted in a non-linear relation between amplitude and load. Fig. 13 provides evidence that the former is true, with different phase locations that have approximately the same amplitude generating differing loads. Without testing with other regular wave frequencies it is not possible to conclude whether the f_1 background had a larger influence than f_2 due to differences in the regular wave steepness or due to its relation to the model's resonance frequencies.

There is a less obvious correlation between the steepness of the CNW and the load (Fig. 14), which is in agreement with the very small effect of crest steepness observed in the first experimental series.

Fig. 15 plots the change in maximum surge with phase position. Unlike with peak mooring load, for the majority of phase locations the maximum surge generated by the CNW was less than that generated by the individual NewWave. There is also a strong dependence on the background regular wave frequency, with the maximum surge generated in the f_2 cases covering a larger range. Comparing Fig. 15 with Fig. 10 it can be observed that there is a correlation between the CNW amplitude and the peak surge for f_2, although not for f_1 (fitting a line of best fit to amplitude against maximum surge data results in an R^2 value of 0.89 for f_2 compared to 0.17 for f_1). This is consistent with the peak load results.

7. Irregular constrained NewWave results

The quality of wave generation was assessed for each of the 180 irregular constrained NewWave by calculating the root mean square error (*RMSE*) between the signal from wave gauge 6 (*WG6*) with the target time series (*TTS*):

$$RMSE = \sqrt{\frac{1}{N}\sum_{i=1}^{N}(WG6_i - TTS_i)^2},$$

where N is the number of samples measured. The average RMSE was 0.028 m, with a standard deviation of 0.003 m. When compared to the H_s of the underlying random sea state (0.288 m) this indicates a relatively good reproduction of the input time signal.

As with the regular cases, the main crest of the CNW is reproduced less well than the underlying irregular sea state. In Fig. 16 the distribution of the measured embedded crest amplitudes are presented, normalised with respect to the NewWave theoretical crest amplitude. The distribution of crest amplitudes is approximately normal, with a standard deviation of 0.155 and a mean of 0.969 of the target crest amplitude. In 97 of the 180 cases measured crest amplitude was within ±10% of the target theoretical amplitude.

A similar comparison of the wave steepness of the embedded focused wave crest with the steepness of the theoretical independent NewWave is shown in Fig. 17.

The mean of this distribution is 1.25, with a standard deviation of 0.42. This distribution has a positive skew of 0.995. Unlike crest amplitude, the focused wave constraining process does not conserve the steepness of the focussed wave groups central crest. The distribution of the target wave steepness had a mean of 1.08, standard deviation of 0.330 and a positive skew of 0.958. It can be observed that, on average, the embedded focused wave was steeper than the initial target.

7.1. Mooring load distribution

The distribution of the peak mooring loads resulting from the 180 irregular CNW are presented in Fig. 18. Loads have been normalised with respect to the peak load produced by the individual NewWave.

The distribution has a mean of 1.11, standard deviation of 0.14 and a skew of 0.22. Comparing Fig. 18 to the distribution of crest amplitude (Fig. 16) and crest steepness (Fig. 17) it cannot be concluded that the

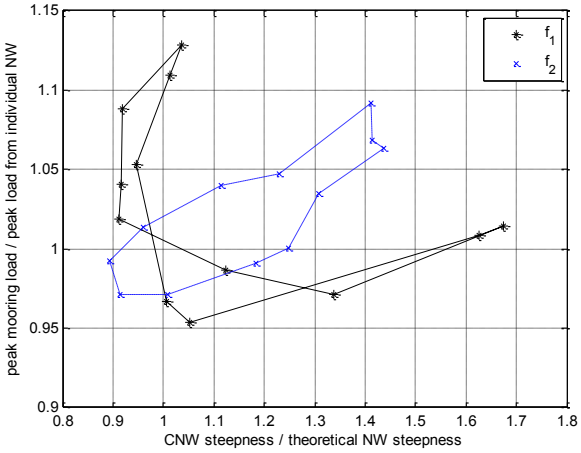

Fig. 14. Variation of peak mooring load generated by CNW with CNW steepness. Plotted lines link neighbouring phase locations.

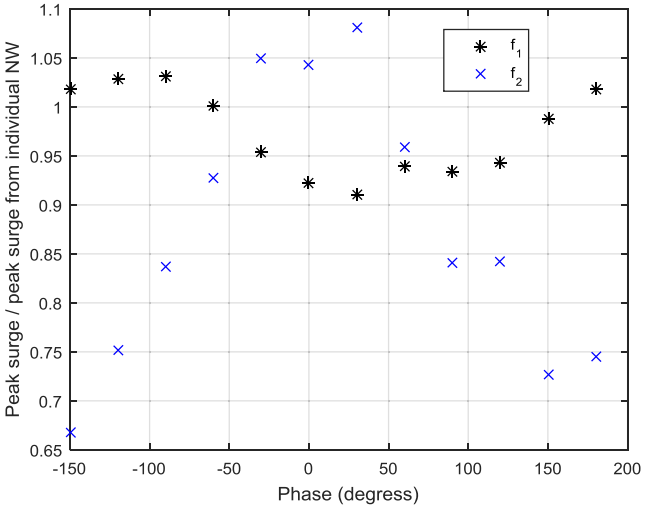

Fig. 15. Variation of peak surge generated by CNW with constraining phase position.

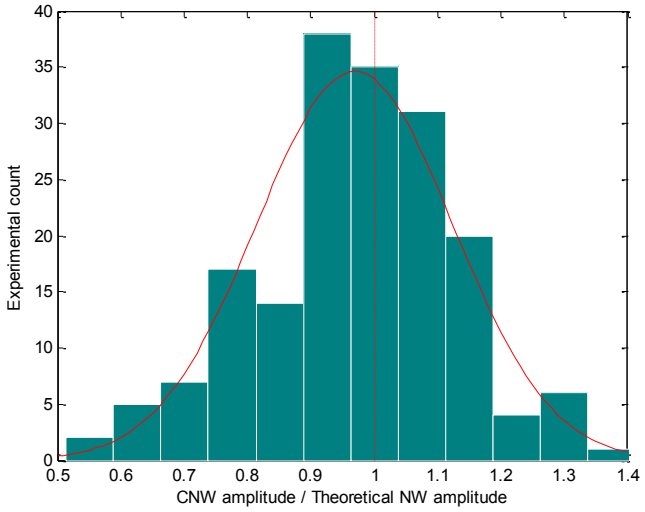

Fig. 16. Distribution of irregular constrained NewWave crest amplitude.

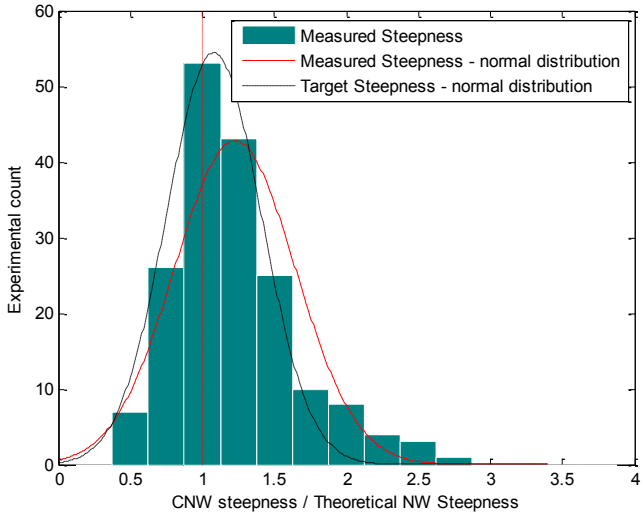

Fig. 17. Distribution of irregular constrained NewWave crest steepness.

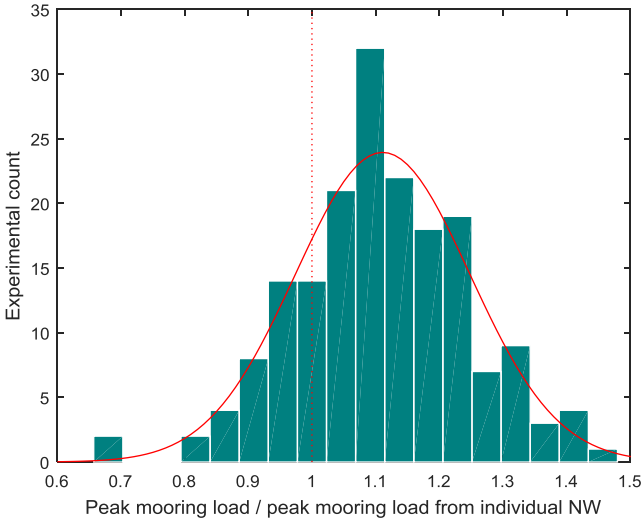

Fig. 18. Distribution of peak mooring load generated by the irregular CNW.

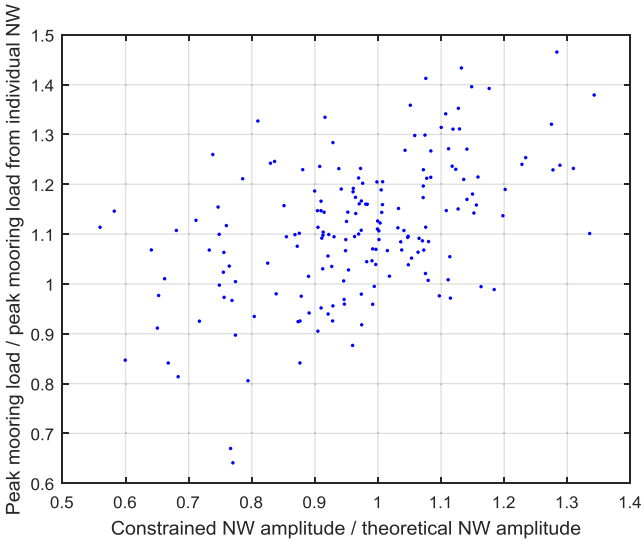

Fig. 19. Peak mooring load generated by irregular CNW plotted against the measured CNW amplitude.

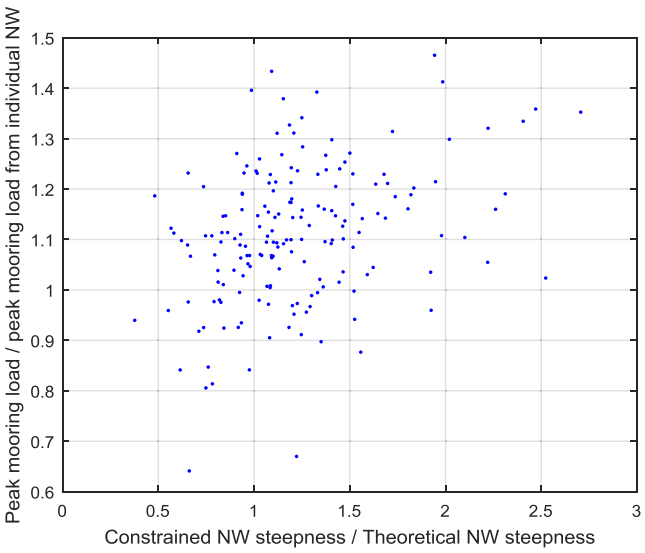

Fig. 20. Peak mooring load generated by irregular CNW plotted against the measured CNW steepness.

observed distribution in mooring load is due to the distribution of the CNW properties. In Figs. 19 and 20 the measured loads are plotted against the normalised crest amplitudes and crest steepnesses respectively. The lack of strong correlation in both figures suggest that the variation in properties of the generated CNW are not the only causes of the distribution in loads. This suggests that the influence of the previous wave field is a significant factor, demonstrating the necessity to consider the influence of this when investigating the interaction between an extreme wave and a moored floating body.

The distribution of the measured maximum surge generated by the CNW is plotted in Fig. 21. As with the other properties this is approximately normal, with a mean of 1.12 of the surge generated by the individual NW, a standard deviation of 0.33 and a skew of −0.076. This larger standard deviation, as compared to the distributions in crest amplitudes and mooring loads, is considered to be an indication that the horizontal excursion of the model is less well predicted by an individual focused wave than the maximum mooring load. It also again emphasises the need to include the influence of the previous wave field when predicting response to an extreme wave.

8. Irregular wave results

A comparison of the results from the two irregular wave experiments with the irregular CNW results identified four cases where the peak mooring load exceeded the largest measured in the CNW cases. These were 1.47, 1.52, 1.53 and 1.60 times the load measured using the individual NewWave, where the largest load measured during the irregular CNW case was 1.465.

The sections of the irregular wave time history that generated these four largest loads are presented in Fig. 22 and are compared with the measured independent NewWave. The time series have been shifted so that the wave crests that generated the large loads occur at $t = 0$. The properties of these four waves have a wide range, with crest amplitude ranging from 0.781 to 1.09 of the target amplitude of the NW and a crest steepness ranging from 1.01 to 2.08 times the steepness of the NW. This further demonstrates the dependence of the mooring load on the previously generated model motions.

The variation between the irregular and CNW cases was less for the measured surge than it was for the mooring loads. The largest measured value of surge was 2.31 times the maximum surge generated by the individual NewWave for the irregular case and 2.23 times from the irregular CNW cases.

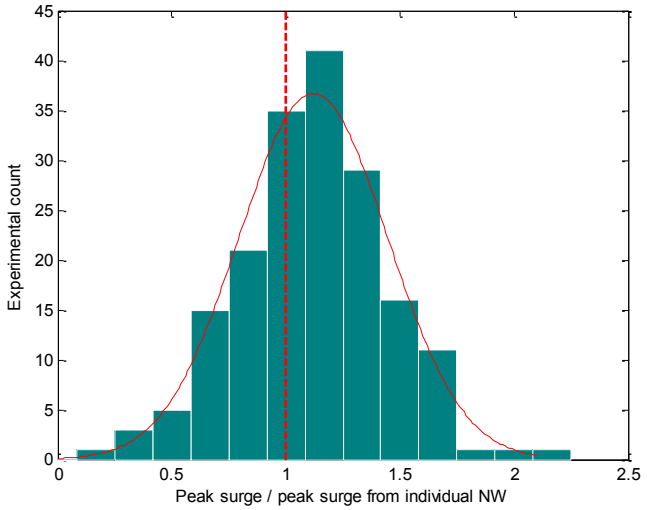

Fig. 21. Distribution of peak surge generated by the irregular CNW.

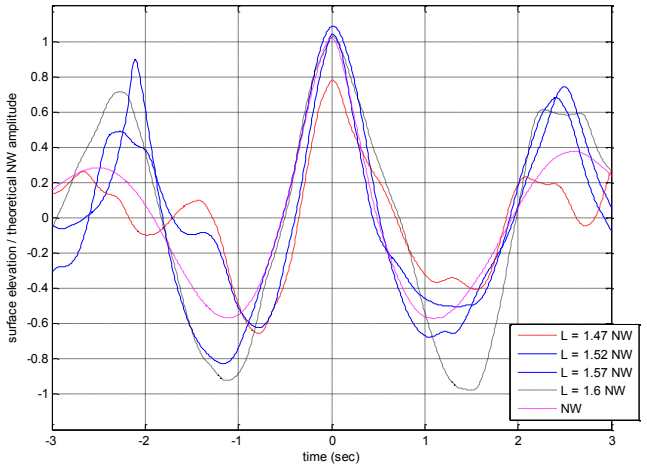

Fig. 22. Waves from the two irregular wave runs which produced mooring loads greater than that measured in the irregular CNW cases.

9. Conclusions

Results are reported from four series of experiments designed to measure the response of a taut moored floating body, representing a point absorbing wave energy converter, to an extreme wave. Tests with individual focused waves based on NewWave theory demonstrated that the steepness of the main crest of the focused wave had negligible effect on the response of the floating body. However the floats motion once the central crest has passed the model showed significant differences resulting from the differences in steepness. This demonstrates the non-linear response of the model, with initially very small changes induced by changes in wave steepness resulting in significantly increased changes in motion once the wave has passed. This is significant when trying to develop methods to predict dynamic model responses to extreme waves as it indicates that even small changes in previous wave conditions could have a significant effect on the position and motion of a model when interacting with the extreme wave.

To explore the effect of a device's load history (as generated by the preceding wave field) on its response to an extreme wave, a NewWave constrained into a series of regular and irregular waves were used. In both cases differences between the target and generated constrained time series have limited the potential benefit of this approach. Bennett et al. (2012) report a similar finding when generating constrained NewWave experimentally. It is potentially feasible that an iterative approach could be used to adjust the wave generator input signal to improve the agreement between the target and generated constrained NewWave. However this would be too time consuming when conducting enough irregular constrained NewWave experiments to draw meaningful conclusions from the results. The impact of this approach on the background sea state is also unknown.

Regardless of the differences between the target and generated time series it is still concluded from the CNW experiments that the use of an independent focused wave is insufficient to properly model the response of a moored floating body such as wave energy converter to an extreme wave. Instead the body's load history must also be modelled.

Comparisons between the irregular and regular CNW cases indicate that it is also insufficient to model this load history using regular waves. Although the use of regular waves allows for a more systematic study, potentially reducing the number of test cases, result here found significantly higher mooring loads and surge levels from the comparable irregular CNW cases. The regular CNW results did demonstrate a dependence on the frequency of the background wave, so it is possible that other frequencies would have generated loads and surges more comparable to the irregular cases. However this seems unlikely considering the range of responses seen for the two frequencies tested here.

Ideally the background wave properties associated with the largest responses to the irregular CNW could be identified and used to limit the number of CNW tests that need to be conducted. Attempts to do this were inconclusive however. As results from the individual focused waves showed, even small changes in a specific wave can result in significant difference later on. Any conclusion that could have been drawn would likely have been device geometry and mooring specific as well, therefore making the use of such an approach limited.

Finally results from the two 3 h long irregular wave runs found 4 times where generated mooring loads were larger than any measured in the CNW cases. With the CNW approach the assumption is made that the NewWave will generate the largest response, with only the changes in the previous sea state being significant. It can be concluded from the irregular wave cases that this is not necessarily the case, and that for a particular sea state the traditional experimental approach of generating a random time series may be the better method of finding the maximum expected load and surge as this assumption is avoided. The random nature of this approach however also requires multiple cases of the full length sea state to be run (as opposed to the shorter time series involved with the CNW approach) to gain greater certainty in what the largest expected responses are. This is prohibitively expensive to do experimentally and indicates that numerical approaches, validated by representative experimental results, might be a better approach.

Acknowledgements

This research was conducted as part of EPRSC project EP/J010235/1, X-MED: Extreme Loading of Marine Energy Devices due to Waves, Current, Flotsam and Mammal Impact. The principal investigator is Professor P.K. Stansby at the University of Manchester.

References

Baldock, T.E., Swan, C., Taylor, P.H., 1996. A laboratory study of nonlinear surface waves on water. Philosophical Transactions of the Royal Society: Mathematical. Phys. Eng. Sci. 354, 649–676.

Barstow, S., Mollison, D., Cruz, J., 2008. The wave energy resource. In: Cruz, J. (Ed.), Ocean Wave Energy - Current Status and Future Perspectives. Springer, Berlin.

Bennett, S.S., Hudson, D.A., Temarel, P., 2012. A comparison of abnormal wave generation techniques for experimental modelling of abnormal wave-vessel interactions. Ocean. Eng. 51, 34–48.

Blanco, M., Moreno-Torres, P., Lafoz, M., Ramirez, D., 2015. Design parameter analysis of point absorber WEC via an evolutionary-algorithm-based dimensioning tool. Energies 8 (10), 11203–11233.

Borthwick, A.G.L., Hunt, A.C., Feng, T., Taylor, P.H., Stansby, P.K., 2006. Flow kinematics of focused wave groups on a plane beach in the U.K. Coastal Research Facility. Coast. Eng. 53, 1033–1044.

Cassidy, M.J., 1999. Non-linear Analysis of Jack-up Structures Subjected to Random Waves (Ph.D. Thesis). University of Oxford, Oxford, UK.
Cassidy, M.J., Eatock Taylor, R., Houlsby, G.T., 2001. Analysis of jack-up units using a Constrained NewWave methodology. Appl. Ocean Res. 23, 221–234.
Enderami, S.M., Zeinoddni, M., Shabakhty, N., Ameryoun, H., 2010. Dynamic non-linear analysis of offshore jacket type platforms under extreme wave loads. In: Proceedings of the ASME 29th International Conference on Ocean, Offshore and Artic Engineering, pp. 593–601. Shanghai, China.
Fernández, H., Sriram, V., Schimmels, S., Oumeraci, H., 2014. Extreme wave generation using self correcting method – revisited. Coast. Eng. 93, 15–31.
Göteman, M., Engström, J., Eriksson, M., Leijon, M., Hann, M., Ransley, E., Greaves, D., 2015. Wave loads on point-absorbing wave energy devices in extreme waves. J. Ocean Wind Energy 2 (3), 176–181.
Halcrow, 2006. South West of England Regional Development Agency: Wave Hub Development and Design Phase Coastal Processes Study Report.
Hann, M., Greaves, D., Raby, A., 2015. Snatch loading of a single taut moored floating wave energy converter due to focused wave groups. Ocean. Eng. 96, 258–271.
Hunt-Raby, A.C., Borthwick, A.G.L., Stansby, P.K., Taylor, P.H., 2011. Experimental measurement of focused wave group and solitary wave overtopping. J. Hydraul. Res. 49 (4), 450–464.
McCabe, A.P., Aggidis, G.A., 2009. Optimum mean power output of a point-absorber wave energy converter in irregular waves. Proc. Inst. Mech. Eng. Part A J. Power Energy 223 (7), 773–781.
Ning, D.Z., Zang, J., Liu, S.X., Eatock Taylor, R., Teng, B., Taylor, P.H., 2009. Free-surface evolution and wave kinematics for nonlinear uni-directional focused wave groups. Ocean. Eng. 36, 1226–1243.
O'Neill, L., Fakas, E., Cassidy, M., 2006. A methodology to simulate floating offshore operations using a design wave. J. Offshore Mech. Arct. Eng. 128 (4), 304–313.
Pinna, R., Cassidy, M., 2004. Dynamic analysis of a monopod platform using constrained NewWave. In: ASME 2004 23rd International Conference on Offshore Mechanics and Artic Engineering. American Society of Mechanical Engineers, pp. 141–148.
Ransley, E., Hann, M., Greaves, D., Raby, A., Simmonds, D., 2013. Numerical and physical modelling of extreme waves at Wave Hub. J. Coast. Res. 1645–1650. Special Issue No. 65.
Rozario, J.B., Tromans, P.S., Efthymiou, M., 1993. Comparison of loads predicted using "NewWave" and other wave models with measurements on the tern structure. In: Wave Kinematics and Environmental Forces. 29, Advances in Underwater Technology, Ocean Science and Offshore Engineering, pp. 143–159.
Stallard, T., Taylor, P.H., Williamson, C.H.K., Borthwick, A.G.L., 2009a. Cylinder loading in transient motion representing flow under a wave group. Proc. R. Soc. A 465, 1467–1488.
Stallard, T.J., Weller, S.D., Stansby, P.K., 2009b. Limiting heave response of a wave energy device by draft adjustment with upper surface immersion. Appl. Ocean Res. 31, 282–289.
Taylor, P.H., Jonathan, P., Harland, L.A., 1997. Time domain simulation of jack-up dynamics with extremes of a Gaussian process. J. Vib. Acoust. 119, 624–628.
Tromans, P.S., Anaturk, A., Hagemeijer, P., 1991. A new model for the kinematics of large ocean waves – application as a design wave. In: The Proceedings of the 1st International Offshore and Polar Engineering Conference, pp. 64–71. Edinburgh, UK.
Walker, D.A.G., Eatock Taylor, R., 2005. Wave diffraction from linear arrays of cylinders. Ocean. Eng. 32, 2053–2078.
Weller, S.D., Stallard, T.J., Stansby, P.K., 2013. Experimental measurements of the complex motion of a suspended axisymmetric floating body in regular and near-focused waves. Appl. Ocean Res. 39, 137–145.
Westphalen, J., Greaves, D.M., Raby, A., Hu, Z.Z., Causon, D.M., Mingham, C.G., Omidvar, P., Stansby, P.K., Rogers, B.D., 2014. Investigation of wave-structure interaction using state of the art CFD techniques. Open J. Fluid Dyn. 4, 18–43.
Whittaker, C.N., Fitzgerald, C.J., Raby, A.C., Taylor, P.H., Orszaghova, J., Borthwick, A.G.L., 2017. Optimisation of focused wave group runup on a plane beach. Coast. Eng. 121, 44–55.
Zang, J., Taylor, P.H., Morgan, G.C.J., Orszaghova, J., Grice, J., Stringer, R., Tello, M., 2010, August. Steep wave and breaking wave impact on offshore wind turbine foundations–ringing re-visited. In: Proc. 25th International Workshop on Water Waves and Floating Bodies. Harbin, China.